

# Synthetic Route Effect on Macromolecular Architecture: From Block to Gradient Copolymers Based on Acryloyl Galactose Monomer Using RAFT Polymerization

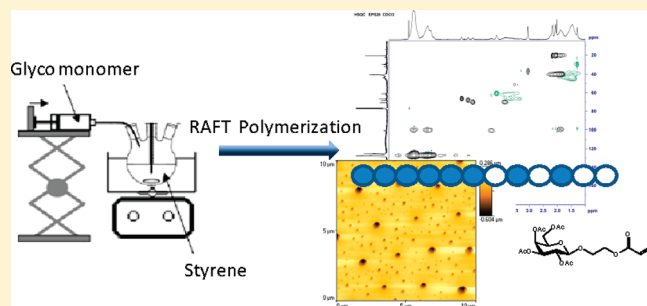
Pierre Escalé,<sup>†,‡</sup> S. R. Simon Ting,<sup>‡</sup> Abdel Khoukh,<sup>†</sup> Laurent Rubat,<sup>†</sup> Maud Save,<sup>†</sup> Martina H. Stenzel,<sup>\*,‡</sup> and Laurent Billon<sup>\*,†</sup>

<sup>†</sup>IPREM Equipe de Physique et Chimie des Polymères, UMR 5254 CNRS, Université de Pau et des Pays de L'Adour, Hélioparc, 2 Avenue du Président Angot, 64053 Pau Cedex, France

<sup>‡</sup>Centre for Advanced Macromolecular Design, School of Chemical Engineering, University of New South Wales, Sydney NSW 2052, Australia

## Supporting Information

**ABSTRACT:** Statistical, gradient, and block copolymer containing 2-(2',3',4',6'-tetra-*O*-acetyl- $\beta$ -D-galactosyloxy)ethyl acrylate (AcGalEA) glycomonomer and styrene (S) were synthesized by RAFT polymerization using *S*-methoxycarbonylphenylmethyl dodecyltrithiocarbonate (MCPDT) as control agent. The block copolymer was synthesized by a two-stage experiment, whereas the statistical and gradient copolymers were obtained in one-pot synthesis. Results obtained from the size exclusion chromatography (SEC) and the nuclear magnetic resonance (NMR) reveal that the polymers synthesized by RAFT were controlled. The kinetic of each synthetic route was investigated, and the reactivity ratio of both monomers was estimated by *in situ* NMR experiments:  $r_{\text{AcGalEA}} = 0.07 \pm 0.01$  and  $r_{\text{S}} = 0.7 \pm 0.1$ . Moreover the AcGalEA moieties were deacetylated to achieve potential amphiphilic bioactive copolymer. The preparation of three different macromolecular architectures to form honeycomb porous films by breath figure process was investigated using atomic force microscopy (AFM).



## INTRODUCTION

In recent years, glycopolymers (i.e., polymers carrying pendant carbohydrate moieties) have received increasing attention due to the numerous biological mechanisms in which carbohydrates are implicated. The biological mechanisms include cell-to-cell recognition, inflammation, signal transmission and infection.<sup>1–4</sup> Glycopolymers could be also used for drug delivery nanoreactors, radio-labeled sugar–nucleotide donors, surfaces modifications, and cell surface receptor.<sup>5–10</sup>

These polymers can be obtained by postpolymerization glycosylation reaction or polymerization of galactose containing monomers.<sup>11–21</sup> Various controlled living polymerization techniques such as ring-opening metathesis polymerization (ROMP),<sup>22,23</sup> living anionic polymerization,<sup>24</sup> nitroxide-mediated radical polymerization (NMP),<sup>18,20,25–29</sup> atom transfer radical polymerization (ATRP),<sup>19,30–34</sup> and reversible addition–fragmentation chain-transfer polymerization (RAFT)<sup>11–15,35–39</sup> were employed for the synthesis of homopolymers, block copolymers, and hyperbranched polymers. To date, only Charreyre et al. reported the synthesis of gradient glycopolymer architectures by the RAFT process.<sup>40</sup> In this work, biotin end-functionalized hydrophilic glycopolymers were synthesized using copolymerization of an

acrylamide galactose derivative with *N*-acryloylmorpholine. Polymer chains with a very slight gradient microstructure were prepared, and reactivity ratio of the monomers was not investigated to control the gradient profile.

In this article, we report for the first time the synthesis of amphiphilic copolymer with a gradient architecture by reversible addition–fragmentation chain-transfer (RAFT) polymerization using a trithiocarbonate control agent (Scheme 1). A comprehensive characterization of the polymer chain architecture was conducted and the synthetic methodology effect on the macromolecular architecture was also investigated. A particular effort in the determination of reactivity ratio of AcGalEA and S monomers was made considering that any values for this kind of monomer are indeed available in the literature.

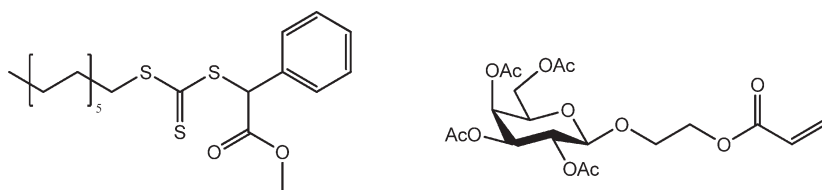
Moreover, we studied the ability of different architectures such as block, statistical, and gradient to form potential bioactive honeycomb porous surface. Highly organized porous surfaces can be obtained by fast evaporation of solvent in appropriate

Received: May 27, 2011

Revised: July 4, 2011

Published: July 14, 2011

**Scheme 1.** Structure of *S*-Methoxycarbonylphenylmethyl Dodecyltrithiocarbonate (MCPDT) RAFT Agent and 2-(2',3',4',6'-Tetra-*O*-acetyl- $\beta$ -D-galactosyloxy)ethyl Acrylate (AcGalEA) Glycomonomer



conditions.<sup>41,42</sup> This simple, inexpensive, and robust bottom-up mechanism of pattern formation is known as the breath figure approach (BFA). This phenomenon occurs when vapor condenses onto a cold solid or liquid surface.<sup>43,44</sup> The created breath figure template can be trapped by a polymer solution yielding to a porous film. The pores are the result of empty water droplets. The regular arrays of pores may be favored by Bénard–Marangoni convection taking place in solution presenting a thermal gradient.<sup>45,46</sup> Several parameters such as polymer concentration, solvent, substrate, inert gas flow, chain-end functionality, and relative humidity can induce the control of pores ordering and diameters.<sup>47–50</sup> Honeycomb films from BFA could find potential applications such as superhydrophobic surface, microelectronic, optoelectronic, photonics, sensors, photovoltaic, and also for biomedical applications.<sup>51–57</sup> Indeed, bioactive moieties that are immobilized onto a surface might serve for protein immobilization or for screening devices.<sup>6,58</sup>

Herein, an acetyl galactosyloxyethyl acrylate (AcGalEA) (Scheme 1) was used considering its potential bioactivity after deacetylation, whereas styrene (S) was chosen as comonomer to afford a sufficient hydrophobic part to the copolymer. Indeed, all the synthesized copolymers were highly hydrophobic in order to favor honeycomb porous film formation. As mentioned in several works on honeycomb porous films, to enhance pore regularity, the hydrophobic fraction in the polymer need to be substantial to ensure the sufficient surface tension of the water droplet and consequently to avoid coalescence of the droplets. AFM analysis was used to reveal the quality of the porous film.

## EXPERIMENTAL SECTION

**Materials.**  $\beta$ -D-Galactose pentaacetate (98%), 2-hydroxyethyl acrylate (HEA, 98%), boron trifluoride diethyl etherate (purum, dist.), and dichloromethane (DCM, 99.5%) were purchased from Aldrich. Ethyl acetate (ACS reagent,  $\geq 99.5\%$ ) and cyclohexane (ACS reagent,  $\geq 99\%$ ) for flash chromatography were used as purchased from Aldrich. Styrene (S, Aldrich, 99%) was freshly deinhibited using an inhibitor remover column from Aldrich before use. 1-Dodecanethiol ( $\geq 98\%$ ), potassium hydroxide (97.0%), carbon disulfide (ACS reagent,  $\geq 99.9\%$ ), methyl  $\alpha$ -bromophenyl acetate (97%), 2,2'-azobis(2-methylpropanitrile) ( $\geq 98\%$ ), and *N,N*-dimethylacetamide (HPLC grade) were also purchased from Aldrich and used directly. Sodium methoxide in methanol (MeONa 0.5 M in MeOH, Aldrich) was used as received.

**Synthesis.** *Synthesis of 2-(2',3',4',6'-Tetra-*O*-acetyl- $\beta$ -D-galactosyloxy)ethyl Acrylate (AcGalEA).*  $\beta$ -D-Galactose pentaacetate (10.0 g,  $2.60 \times 10^{-2}$  mol) and 2-hydroxyethyl acrylate HEA (6.0 mL, 0.052 mol) were introduced into a 250 mL round-bottom flask with dried 3 Å molecular sieves. Dichloromethane (100 mL) was dried overnight and introduced in the flask, and the mixture was purged under nitrogen for 30 min. Then, boron trifluoride (16.0 mL, 0.129 mol) was slowly added during 30 min while maintaining the flow of nitrogen through the flask.

Reaction was left for 48 h. The final suspension was filtered in order to remove the molecular sieves and washed three times with saturated salt solution. The resulting organic phase was removed under reduced pressure and purified by flash chromatography using 254 nm UV detection and cyclohexane/ethyl acetate (3:2) as eluent. The final solution was placed under reduced pressure for 48 h. Purity of the crystallized product was confirmed by mass spectroscopy and  $^1\text{H}$  NMR (see Figures SI-1 and SI-2 in Supporting Information). ESI-MS (in methanol) calculated for  $\text{C}_{19}\text{H}_{30}\text{O}_{12}\text{N} + \text{NH}_4^+$   $m/z$ , 464.20; found,  $m/z$  464.18.  $^1\text{H}$  NMR ( $\text{CDCl}_3$ , 400 MHz)  $\delta$  (ppm): 1.98, 2.02, 2.05, 2.15 (s, 12H, 4  $\text{CH}_3$ ), 4.53 (d, anomeric 1H), 5.0, 5.2 (dd, 2H, CH sugar moiety), 5.4 (d, 1H, CH sugar moiety), 5.8 (m, 1H, vinylic H), 6.1 (m, 1H, vinylic H), 6.4 (m, 1H, vinylic H).  $^{13}\text{C}$  NMR ( $\text{CDCl}_3$ , 400 MHz)  $\delta$  (ppm): 20.56, 20.64 (s, 12C, 4  $\text{CH}_3$ ), 61.27 (s, 1C,  $\text{CH}_2-\text{C}(\text{O})=\text{O}$ ), 63.27 (s, 1C,  $\text{CH}_2-\text{CH}_2-\text{C}(\text{O})=\text{O}$ ), 66.98, 68.61, 70.84 (s, 3C, sugar moiety CH), 67.41 (s, 1C,  $\text{CH}-\text{CH}_2-\text{OCH}_3$ ), 101.29 (s, 1C,  $\text{O}-((\text{CH}_2)_2)-\text{O}-\text{CH}$ ), 128.08 (s, 1C,  $\text{CH}_2=\text{CH}$ ), 130.27 (s, 2C,  $\text{CH}_2=\text{CH}$ ), 166.12 (s, 1C,  $\text{C}(\text{O})=\text{O}$ ).

*Synthesis of S-Methoxycarbonylphenylmethyl Dodecyltrithiocarbonate (MCPDT).* MCPDT RAFT agent was synthesized as reported previously with slight modifications.<sup>59</sup> 1-Dodecanethiol (6.41 g,  $3.17 \times 10^{-2}$  mol) was suspended in 43 mL of distilled water and cooled in an ice bath. This was followed by the addition of potassium hydroxide (1.82 g,  $3.25 \times 10^{-2}$  mol) before 6.5 mL of carbon disulfide was introduced dropwise into the suspension. A yellow emulsion was observed during the addition of carbon disulfide. Methyl *R*-bromophenyl acetate (5.0 g,  $2.19 \times 10^{-2}$  mol) was eventually added dropwise into the yellow emulsion, and a condenser was attached onto the single neck round-bottom flask, after which the reaction vessel was heated to 80 °C for 12 h. Upon cooling, the water phase was separated from the organic phase and washed with methylene chloride ( $3 \times 20$  mL). The yellow solution of all the organic phases were concentrated under reduced pressure to give a yellow oil. The yellow oil was further purified through a column using toluene as the eluent with the product exiting at an  $R_f$  value of 0.8. The combined fractions were dried under reduced pressure and high vacuum to yield a bright yellow oil and upon cooling in the fridge gave a bright yellow solid. The reaction conversion (60%) was obtained using  $^1\text{H}$  NMR by observing the integrals from the proton shift of 4.51 to 5.75 ppm. ESI-MS ( $\text{CH}_2\text{Cl}_2$ ) calculated for  $\text{C}_{22}\text{H}_{34}\text{O}_2\text{S}_3 + \text{Ag}^+$   $m/z$ , 533.08; found,  $m/z$  533.30.  $^1\text{H}$  NMR ( $\text{CDCl}_3$ , 300 MHz)  $\delta$  (ppm): 0.81 (t, 3H,  $\text{CH}_3$ ), 1.19 (s, 18H,  $\text{CH}_3-\text{C}_9\text{H}_{18}-(\text{CH}_2)_2-\text{S}$ ), 1.61 (m, 2H,  $\text{CH}_2-\text{CH}_2-\text{S}$ ), 3.26 (t, 2H,  $\text{CH}_2-\text{S}$ ), 3.68 (s, 3H,  $\text{O}-\text{CH}_3$ ), 5.75 (s, 1H,  $\text{S}-\text{CH}(\text{Ph})-\text{C}(\text{O})=\text{O}$ ), 7.27 (m, 5H,  $\text{ArH}_5$ ).  $^{13}\text{C}$  NMR ( $\text{CDCl}_3$ , 75.5 MHz)  $\delta$  (ppm): 14.53 (1C,  $\text{CH}_3$ ), 23.09 (1C,  $\text{CH}_3-\text{CH}_2$ ), 28.23, 29.30, 29.48, 29.74, 29.82, 29.94, 30.02, 30.11 (8C,  $\text{C}_8\text{H}_{16}-\text{CH}_2-\text{S}$ ), 32.32 (1C,  $\text{CH}_3-\text{CH}_2-\text{CH}_2$ ), 37.72 (1C,  $\text{CH}_2-\text{S}$ ), 53.60 (1C,  $\text{O}-\text{CH}_3$ ), 58.19 (1C,  $\text{S}-\text{CH}(\text{Ph})-\text{C}(\text{O})=\text{O}$ ), 125.70, 128.62, 129.15, 129.29, 129.44, 133.64 (6C,  $\text{ArC}$ ), 169.90 (1C,  $\text{CH}(\text{Ph})-\text{C}(\text{O})=\text{O}$ ), 222.40 (1C,  $\text{S}=\text{C}(\text{S})-\text{S}$ ).

*RAFT Polymerization of AcGalEA First Block (Experiment 3 in Table 1).* AcGalEA ( $4.5 \times 10^{-1}$  g,  $1.0 \times 10^{-3}$  mol) and MCPDT ( $4.3 \times 10^{-3}$  g,  $1.0 \times 10^{-5}$  mol) were introduced into a 5 mL one-neck round-bottom

**Table 1.** Experimental Conditions for the Synthesis of PS-*b*-PACGalEA, PS-*co*-PACGalEA, and PS-*b*-P(AcGalEA-*grad*-S) by RAFT Polymerization Using MCPDT as Control Agent

expt	polymer	<i>T</i> (°C)	[AcGalEA] <sub>0</sub> (mol L <sup>-1</sup> )	[S] <sub>0</sub> (mol L <sup>-1</sup> )	[CTA] <sub>0</sub> <sup>a</sup> (mol L <sup>-1</sup> )	[AIBN] <sub>0</sub> (mol L <sup>-1</sup> )	time (min)	conv (%)	<i>M</i> <sub>n</sub> (SEC, calib PS) (g mol <sup>-1</sup> )	<i>M</i> <sub>w</sub> / <i>M</i> <sub>n</sub>
1 <sup>c</sup>	PACGalEA	90	0.70		$7.10 \times 10^{-3}$	$8.7 \times 10^{-4}$	145	82	15 720	1.21
2 <sup>c</sup>	PACGalEA	70	0.70		$6.90 \times 10^{-3}$	$1.7 \times 10^{-3}$	480	94	16 220	1.15
3 <sup>c</sup>	PACGalEA	60	0.69		$6.90 \times 10^{-3}$	$2.7 \times 10^{-3}$	960	88	14 520	1.17
4 <sup>c</sup>	PACGalEA- <i>b</i> -PS	60		2.16	$4.37 \times 10^{-3}$	$1.8 \times 10^{-3}$	1200	17	16 150	1.57
5 <sup>b</sup>	PS	90		8.14	$4.54 \times 10^{-2}$	$5.3 \times 10^{-3}$	360	50	7 560	1.23
6 <sup>c</sup>	PS- <i>b</i> -PACGalEA	90	0.58		$1.15 \times 10^{-2}$	$1.4 \times 10^{-3}$	200	18	10 320	1.32
7 <sup>c</sup>	PS- <i>co</i> -PACGalEA	90	1.59	6.36	$3.66 \times 10^{-2}$	$4.7 \times 10^{-3}$	1440	55 <sup>d</sup>	13 300	1.26
8 <sup>c</sup>	PS- <i>b</i> -P(AcGalEA- <i>grad</i> -S)	90		8.16	$4.3 \times 10^{-2}$	$5.1 \times 10^{-3}$	450	53 <sup>S</sup> /36 <sup>AcGalEA</sup>	10 270	1.18

<sup>a</sup>[CTA]<sub>0</sub> corresponds to the initial concentration of chain transfer agent which is MCPDT RAFT agent in the case of experiments 1, 2, 3, 5, 7, and 8; PACGalEA macro-RAFT agent in the case of experiment 4 and PS macro-RAFT agent for experiment 6. <sup>b</sup>Polymerization was carried out in bulk. <sup>c</sup>Polymerization was carried out in DMAc. <sup>d</sup>The conversion corresponds to the global conversion.

flask. AIBN was introduced by first preparing a solution of AIBN in DMAc ( $7.2 \times 10^{-3}$  g in 1 mL) and taking the appropriate quantity (91 μL). Then DMAc (9 mL) was added to dissolve the mixture. The solution was degassed for 45 min using nitrogen and introduced into a preheated oil bath at 60 °C. At the end of the polymerization, a part of the crude solution was dissolved in CDCl<sub>3</sub> for <sup>1</sup>H NMR analysis. AcGalEA conversion was determined using the integration of a monomer vinylic proton at 6.15 ppm with the integration of the CH from the galactose of both monomer and polymer ( $3H_{\text{monomer}} + 3H_{\text{polymer}} + 1H_{\text{styrene}}$ , 5.7–7.6 ppm). Finally, the resulting PACGalEA block was purified by precipitation in diethyl ether and dried overnight under reduce pressure.

*Chain Extension of PACGalEA Macro-RAFT Agent with S (Experiment 4 in Table 1).* PACGalEA macro-RAFT agent ( $6.9 \times 10^{-2}$  g,  $4.75 \times 10^{-6}$  mol, *M*<sub>n</sub>(SEC,PS calibration) = 14 520 g mol<sup>-1</sup>, *M*<sub>w</sub>/*M*<sub>n</sub> = 1.17) and S ( $1.75 \times 10^{-1}$  g,  $1.7 \times 10^{-3}$  mol) were introduced into a 5 mL one-neck round-bottom flask. AIBN ( $2.6 \times 10^{-3}$  g) was dissolved in DMAc (1 mL), and the appropriate amount of this solution was introduced in the flask (85.7 μL). The reaction mixture was degassed with nitrogen for 45 min and subsequently introduced into an oil bath at 60 °C. At the end of the polymerization a part of the crude solution was withdrawn to determine S conversion by <sup>1</sup>H NMR. S conversion was calculated using the integration of the vinylic protons ( $2H_{\text{monomer}}$ , 5.0–5.7 ppm) of the monomer with the integration of the aromatic protons of both monomer and polymer ( $6H_{\text{monomer}} + 5H_{\text{polymer}}$ , 6.1–7.3 ppm). The resulting PACGalEA-*b*-PS was purified by precipitation in diethyl ether, filtered, and dried under reduced pressure overnight.

*RAFT Polymerization of S First Block (Experiment 5 in Table 1).* S (1.2 g,  $1.2 \times 10^{-2}$  mol) and MCPDT ( $2.9 \times 10^{-2}$  g,  $6.5 \times 10^{-5}$  mol) were measured into a 5 mL one-neck round-bottom flask. A solution of AIBN in DMAc was prepared by dissolving  $1.32 \times 10^{-2}$  g of AIBN in  $9.60 \times 10^{-1}$  g of DMAc. The sufficient quantity of this solution (0.09 g) was withdrawn and introduced into the flask. The reaction mixture was thoroughly degassed for 45 min using nitrogen before it was sealed and placed into a preheated oil bath at 90 °C. Several aliquots were withdrawn at time intervals during polymerization and directly dissolved in CDCl<sub>3</sub> for conversion determination using <sup>1</sup>H NMR analysis. S conversion was calculated using the integration of the vinylic protons ( $2H_{\text{monomer}}$ , 5.0–5.7 ppm) of the monomer with the integration of the aromatic protons of both monomer and polymer ( $6H_{\text{monomer}} + 5H_{\text{polymer}}$ , 6.1–7.3 ppm). The final PS-macro-RAFT agent was purified by precipitation in methanol, filtered, and dried under reduced pressure at room temperature for 48 h before using it as a macro-RAFT agent.

*Chain Extension of PS Macro-RAFT Agent with AcGalEA (Experiment 6 in Table 1).* Purified PS from experiment 3 ( $8 \times 10^{-2}$  g,  $8 \times 10^{-6}$  mol, *M*<sub>n</sub>(SEC,PS calibration) = 7560 g/mol, *M*<sub>w</sub>/*M*<sub>n</sub> = 1.23) and AcGalEA (0.18 g,  $4 \times 10^{-4}$  mol) were measured into a 5 mL one-neck round-bottom flask. A solution of AIBN in DMAc was first prepared by dissolving  $1.58 \times 10^{-2}$  g of AIBN in 2.0 g of DMAc. Then 0.02 g of the freshly prepared solution and 0.62 g of DMAc were added to the flask. After purging the mixture under nitrogen for 45 min, the flask was introduced in a preheated oil bath at 90 °C for 200 min. At the end of the reaction, a part of the crude solution was analyzed in <sup>1</sup>H NMR. AcGalEA conversion was calculated using the integration of one monomer vinylic proton at 6.15 ppm with the integration of the CH from the galactose of both monomer and polymer ( $3H_{\text{monomer}} + 3H_{\text{polymer}} + 1H_{\text{styrene}}$ , 5.7–7.6 ppm). The remaining solution was purified two times by precipitation in methanol and subsequently dried under reduce pressure overnight to yield a slightly yellow powder.

*RAFT Copolymerization of Styrene and AcGalEA (Experiment 7 in Table 1).* In a typical experiment, AcGalEA (1.0 g,  $2.3 \times 10^{-3}$  mol), styrene (0.94 g,  $9.0 \times 10^{-3}$  mol), and MCPDT ( $2.2 \times 10^{-2}$  g,  $5.2 \times 10^{-5}$  mol) were introduced in a 5 mL one-neck round-bottom flask. Moreover, a solution of AIBN ( $1.7 \times 10^{-2}$  g) was first prepared in DMAc (1.98 g). Then the appropriate amount of AIBN was introduced in the flask, and 0.23 g of DMAc was also added. To follow the kinetic polymerization, several aliquots at time intervals were withdrawn and subsequently characterized by <sup>1</sup>H NMR in order to determine individual conversion of both monomers. The final crude solution was precipitated in methanol, filtered, and dried under reduced pressure overnight, yielding to a slightly yellow fine powder.

*Synthesis of Gradient Copolymer Made of Styrene and AcGalEA (Experiment 8 in Table 1).* In a first step styrene (1.04 g,  $1 \times 10^{-2}$  mol) and MCPDT ( $2.3 \times 10^{-2}$  g,  $5.3 \times 10^{-5}$  mol) were introduced in a 10 mL one-neck round-bottom flask. Then, a solution of AIBN ( $1.3 \times 10^{-2}$  g) in DMAc (0.96 g) was prepared, and the appropriate amount was introduced into the flask. The reaction mixture was thoroughly purged with nitrogen for 45 min and sealed. Polymerization was carried out at 90 °C, and aliquots were taken at periodic intervals for the determination of styrene conversion. During the homopolymerization of styrene, a solution of AcGalEA (1.0 g,  $2.3 \times 10^{-3}$  mol) in DMAc (2.1 g) was purged and subsequently withdrawn in a syringe. At the end of a defined time of the stage one, the solution of AcGalEA in DMAc was slowly added using a pump with a rate of 0.5 mL h<sup>-1</sup>. After 4 h 30 min, the addition of the solution was complete, and the reaction was left for 1 h. Several aliquots were taken along and after the addition of the solution in order to monitor the conversion

**Table 2. Experimental Conditions for  $^1\text{H}$  NMR in Situ Experiment for Conventional Copolymerization of AcGalEA and Styrene Using AIBN as Initiator**

expt	$[\text{AcGalEA}]_0$ ( $\text{mol L}^{-1}$ )	$[\text{S}]_0$ ( $\text{mol L}^{-1}$ )	$[\text{AIBN}]_0$ ( $\text{mol L}^{-1}$ )
1	0.62	1.35	0.02
2	0.21	1.93	0.02
3	1.00	1.06	0.02
4	1.65	0.42	0.02

of both styrene and AcGalEA monomers using  $^1\text{H}$  NMR in  $\text{CHCl}_3$ . The final solution was purified by precipitation in methanol, and the resulting solid was isolated by vacuum filtration and dried for 48 h under vacuum, yielding a fine and slightly yellow powder.

**NMR in Situ Copolymerization of AcGalEA and Styrene for Reactivity Ratio Determination (Experiments 1–4 in Table 2).** In experiment 1, AcGalEA ( $0.14 \text{ g}$ ,  $3 \times 10^{-4} \text{ mol}$ ) and styrene ( $0.07 \text{ g}$ ,  $6.8 \times 10^{-4} \text{ mol}$ ) were introduced into a hemolyse tube. AIBN was prepared by first dissolving  $1.7 \times 10^{-2} \text{ g}$  of purified AIBN in  $2 \text{ g}$  of DMAc and transferring  $0.2 \text{ g}$  into the reaction mixture. For this in situ experiment, two NMR tubes were used. The first one which contains the purged reaction mixture was introduced in the second tube which contains the deuterated DMSO. The tubes were sealed with rubber septa and subsequently introduced in the NMR apparatus preheated at  $90^\circ\text{C}$ . By the same method, several kinetics were performed with different  $[\text{AcGalEA}]_0/[\text{S}]_0$  ratio (Table 2).

**Deacetylation.** A solution of purified copolymer from experiment 4, 5, or 6 in Table 1 ( $3 \times 10^{-6} \text{ mol}$ ) in a mixture of  $\text{CHCl}_3$ – $\text{CH}_3\text{OH}$  (1:1,  $8 \text{ mL}$ ) was degassed at room temperature under nitrogen for 30 min. Then,  $1 \text{ mL}$  of a freshly prepared  $1 \text{ M}$  solution of NaOMe in MeOH was added. After  $\sim 10 \text{ s}$ , a white precipitate was observed and disappeared straight away. The reaction was left for 1 h, and the solvents were reduce under reduced pressure. Then, the final solution was purified by precipitation in methanol, filtered, and dried, yielding a fine powder.  $^1\text{H}$  NMR and FTIR were used to confirm that the successful deprotection of acetyl groups on the galactose moieties.

**Honeycomb Film Preparation.** The preparation of the honeycomb film using the breath figure method was conducted in a Perspex glovebox with relative humidity between 35 and 40% at room temperature ( $22$ – $25^\circ\text{C}$ ). The humid air flow was set at  $2 \text{ L min}^{-1}$ . For each copolymer, two series of solution were prepared: (1) copolymers in  $\text{CS}_2$  at  $5 \text{ g L}^{-1}$  and (2) a copolymer/linear PS ( $M_n = 20\,000 \text{ g mol}^{-1}$ ) mixture (1:1, w/w) in  $\text{CS}_2$  at  $5 \text{ g L}^{-1}$ . For the film formation,  $100 \mu\text{L}$  of the solutions was cast on a glass substrate in the Perspex box.

**Analysis. Nuclear Magnetic Resonance (NMR) Spectroscopy.** NMR spectra were recorded using a Bruker 400 MHz spectrometer at  $25^\circ\text{C}$ .  $^1\text{H}$  and  $^{13}\text{C}$  measurements were performed at frequencies of 400.13 and 100.6 MHz, respectively. Deuterated chloroform  $\text{CDCl}_3$  was used as solvent.

**Mass Spectrometry.** Mass spectra were recorded using a LTQ-FTMS Orbitrap VELOS from Thermofisher (precision  $<3 \text{ ppm}$ ). The sample was dissolved in methanol before the characterization.

**Size Exclusion Chromatography (SEC).** Characterizations of the polymers were performed at  $30^\circ\text{C}$  with THF as eluent at a flow rate of  $1 \text{ mL min}^{-1}$ . The SEC system was equipped with three Waters Styragel columns HR 0.5, 2, and 4 working in series (separation range  $1 \times 10^2$ – $3 \times 10^6 \text{ g mol}^{-1}$ ) and a refractive index detector ERC 7515-A. The number-average molar molecular weight ( $M_n$ ) and the dispersity ( $D = M_w/M_n$ ) were derived against a calibration derived from PS standards. All polymers samples were prepared at  $5 \text{ g L}^{-1}$  concentrations and filtered through PVDF  $0.45 \mu\text{m}$  filters.

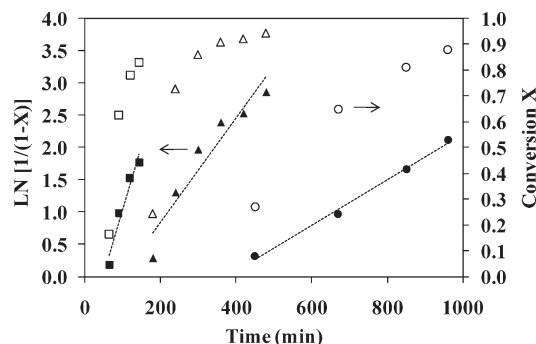


**Figure 1.** Pseudo-first-order kinetic (closed symbol) and conversion plot (open symbol) for the RAFT polymerization of AcGalEA in DMAc using MCPDT at different temperatures: (■)  $90^\circ\text{C}$ , (▲)  $70^\circ\text{C}$ , and (●)  $60^\circ\text{C}$  (experiments 1, 2, and 3 in Table 1).  $[\text{AcGalEA}]/[\text{MCPDT}] = 100$  for each kinetic.

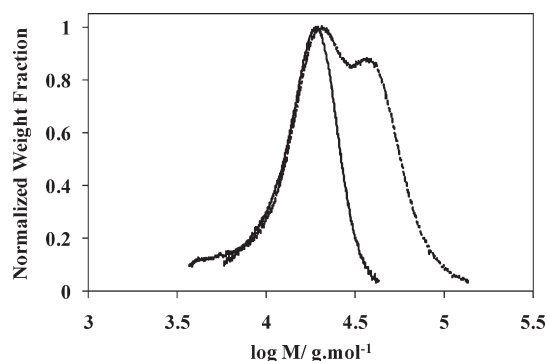


**Figure 2.** Size exclusion chromatograms of PAcGalEA macro-RAFT agent and of the resulting PAcGalEA-*b*-PS obtained in DMAc at  $60^\circ\text{C}$  (experiment 4 in Table 1).

**Atomic Force Microscopy (AFM).** Measurements were performed with an Innova AFM (Veeco Instrument Inc.). The images were scanned in tapping mode under ambient conditions and recorded either as topography images (Figure 9). Rectangular silicon cantilevers from Veeco-probes (MMP-12100–10) with a resonance frequency of about  $150 \text{ kHz}$  were used.

**Optical Microscopy.** Pictures were taken in reflection with a Leica DM/LM microscope equipped with  $\times 50$  optic and a Leica DFC280 video camera. The regular image treatments were performed with the Image Manager IM50 software.

## RESULTS AND DISCUSSION

**Synthesis of Block Copolymer.** Two synthetic approaches were investigated for the synthesis of block copolymers. First, homopolymerization kinetics of AcGalEA using MCPDT and AIBN at different temperatures was performed. Inhibition periods were observed for all three temperature performed (Figure 1). Nevertheless, this period decrease from 320 min at  $60^\circ\text{C}$  to 100 min at  $70^\circ\text{C}$  and, finally, to 50 min at  $90^\circ\text{C}$ . Moreover, we performed the chain extension of a PAcGalEA first block ( $M_n = 14\,500 \text{ g/mol}$ ,  $M_w/M_n = 1.17$ ) in DMAc at  $60^\circ\text{C}$  with styrene. SEC chromatograms of this chain extension showed that the reinitiation of the PAcGalEA first block is not completed (Figure 2). Considering the problem of reinitiation, we also investigated the synthesis of a PS first block and subsequently chain extended with AcGalEA. The homopolymerization

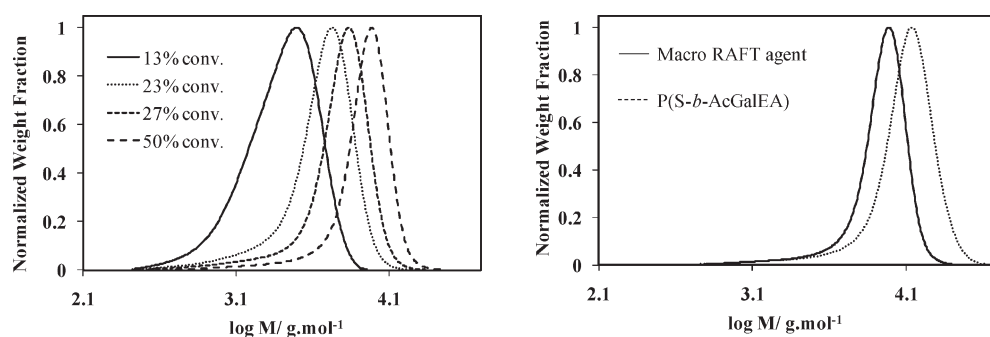


**Figure 3.** Size exclusion chromatograms of PS obtained at different monomer conversion during the polymerization of styrene in bulk at 90 °C (experiment 5 in Table 1) (left). Size exclusion chromatograms of PS macro-RAFT agent and of the resulting PS-*b*-PacGalEA obtained in DMAc at 90 °C. Experimental conditions of experiment 6 are reported in Table 1.

of styrene using MCPDT and AIBN in bulk at 90 °C was controlled as a constant radical concentration with time and a linear dependence of the molecular weight with conversion were observed (see Figure SI-3 in Supporting Information). The SEC chromatograms of PS samples shifted toward high molecular mass with increasing conversion (Figure 3, left). Moreover, the SEC traces of the chain extension of this PS macro-RAFT agent did not show any shoulder, indicating a better reinitiation in comparison to the chain extension of a PacGalEA first block (Figure 3, right). One explanation could be that during the pre-equilibrium of the RAFT process the R radical formed was more stable in the case of the reinitiation of PS as the phenyl group stabilizes the radical, whereas in the case of a PacGalEA chain extension polymerization the radical might be destabilized by the presence of the attractive carboxyl group.<sup>60</sup>

**One-Pot Synthesis of Gradient Copolymers.** Studies have shown that amphiphilic block copolymers are able to form honeycomb porous film using the appropriate conditions and also to create hierarchically structured porous film at the nano- and micrometer scale.<sup>61,62</sup> The final aim of this work was to develop a new methodology to synthesize bioactive polymer in one-pot synthesis, which is time- and cost-saving in comparison to the usual two-step procedure for the synthesis of block copolymer. Nonetheless, the synthesized copolymer needs to be able to form porous structure via the breath figure process. One-pot synthesis of gradient copolymers requires the knowledge of the reactivity ratios of monomers. Indeed, considering two monomers A and B with the corresponding reactivity ratios  $r_A$  and  $r_B$ , the consumption rate for each monomer is driven by the Mayo–Lewis equation:

$$\frac{df_1}{df_2} = \frac{r_1 f_1^2 + f_1 f_2}{r_2 f_2^2 + f_1 f_2} = \frac{F_1}{F_2} \quad (1)$$

Depending on the reactivity ratios and on the initial fraction for both monomers, the instantaneous copolymer composition is affected.<sup>63</sup>

The reactivity ratios of both monomers have not been studied, and no values of the reactivity ratios are available in the literature. Considering that, we investigated the reactivity of both monomers using in situ NMR experiments. Experiments were conducted in several initial mixtures of S and AcGalEA; we followed the kinetics in conventional radical polymerization using AIBN at 90 °C (Figure SI-4A).

The monomer reactivity ratios were estimated with the Skeist equation but also with the Fineman–Ross and Kelen–Tudos

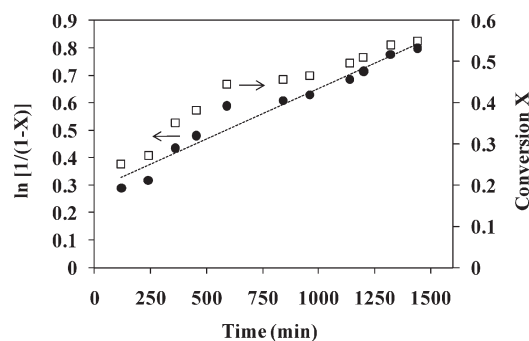


**Figure 4.** Pseudo-first-order kinetic (●) and conversion plots (□) of RAFT copolymerization of styrene and AcGalEA in DMAc at 90 °C using MCPDT as control agent and AIBN as initiator. The experimental conditions are reported in Table 1.

methods.<sup>64–66</sup> The evolution of the AcGalEA monomer fraction versus the global conversion along the copolymerization is shown in Figure SI-4A. For the Skeist method this evolution was fitted for each initial composition in order to determine the reactivity ratios. The monomer reactivity ratios for the AIBN conventional radical copolymerization of S and AcGalEA were  $r_S = 0.7 \pm 0.1$  and  $r_{AcGalEA} = 0.07 \pm 0.01$ . These values reveal that styrene is much more reactive than the glycomonomer. The profile of  $F_S$  in function of the initial composition in styrene monomer  $f_S$  is shown Figure SI-4B. Considering the reactivity ratio obtained and also that a high hydrophobic fraction is required for honeycomb film formation in order to reduce the surface tensions of the water droplet during the breath figure mechanism, spontaneous gradient copolymer with this requirement could not be obtained. Indeed, with an initial fraction of S close to 80%, the composition of the obtained copolymer will be 80% in PS due to the azeotropic curve. The RAFT copolymerization of S (80 mol %) and AcGalEA (20 mol %) was investigated using MCPDT as chain transfer agent and AIBN as initiator in DMAc at 90 °C (experiment 5 Table 1). The first-order kinetic plot shows a linear plot with a high concentration of radical generated at the beginning of the reaction (Figure 4).

Moreover, the evolution of the number-average molecular weight with conversion increases linearly showing a controlled polymerization as the growing chains were constant through the reaction (Figure 5). The molecular weights were determined using PS calibration. This can explain the observed deviation with the theoretical values given that the

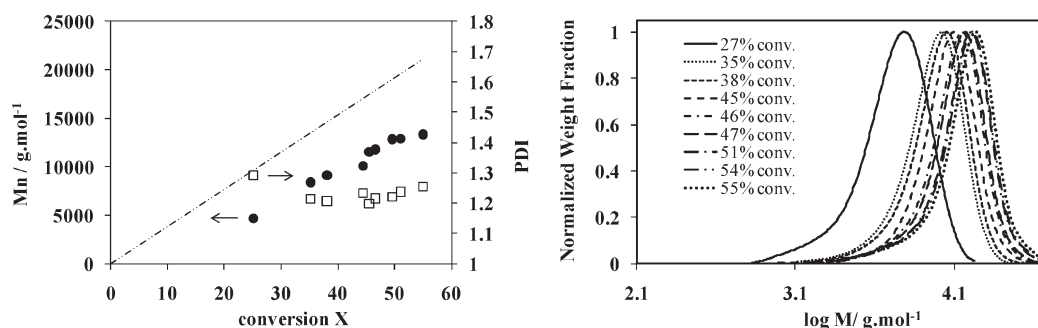


**Figure 5.** Evolution of number-average molar mass for P(AcGalEA-co-S) vs conversion ( $X$ ). Dotted line is the theoretical  $M_n$ , (●) represents the  $M_n$  using PS calibration, and (□) represents the polydispersity index (PDI) (left). Size exclusion chromatograms of P(AcGalEA-co-S) obtained at different monomer conversion during the copolymerization of S and AcGalEA in bulk at 90 °C (right).

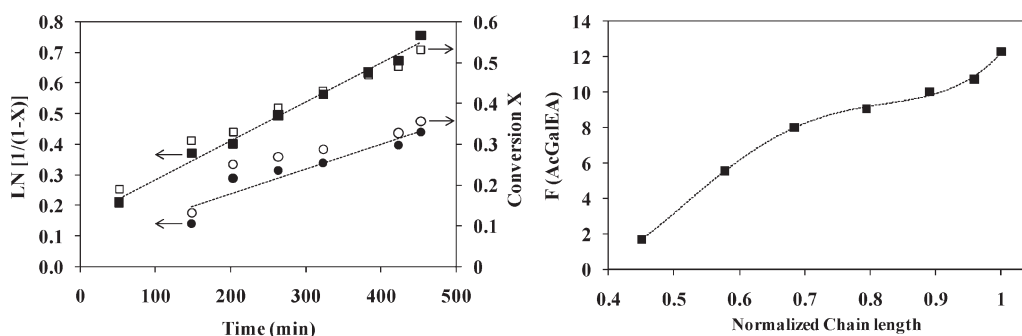


**Figure 6.** Pseudo-first-order kinetic of styrene (■) and AcGalEA (●) and conversion plots of styrene (□) and AcGalEA (○) of RAFT copolymerization of styrene and AcGalEA in DMAc at 90 °C using MCPDT as control agent and AIBN as initiator (left). Instantaneous fraction of AcGalEA in the copolymer as a function of the normalized chain length (right). The experimental conditions are reported in Table 1.

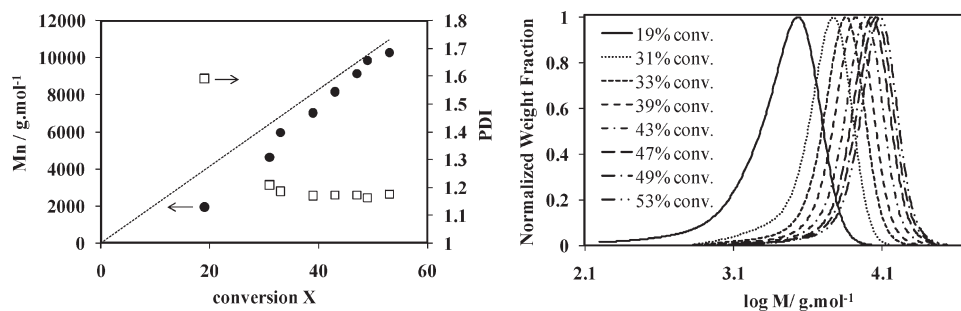


**Figure 7.** Evolution of number-average molar mass for PS-b-P(AcGalEA-grad-S) vs conversion ( $X$ ). Dotted line is the theoretical  $M_n$ , (●) represents the  $M_n$  using PS calibration, and (□) represents the polydispersity index (PDI) (left). Size exclusion chromatograms of PS-b-P(AcGalEA-grad-S) obtained at different monomer conversion during the copolymerization of styrene and AcGalEA in bulk at 90 °C (right).

hydrodynamic volume of the AcGalEA units differs largely from the styrene units.<sup>29</sup>

The final purified copolymer is composed of 15% of AcGalEA monomer units. As expected, the final composition was closed to the initial composition in AcGalEA monomer. In conclusion from this part, gradient profile composition could not be obtained by batch polymerization with aim to have a highly hydrophobic chain. Nevertheless, considering the high difference in reactivity of both monomers, hydrophilic spontaneous gradient copolymer could be obtained and will be the objective of future research. Indeed in this case, the hydrophilic copolymer could be used as a model for micellization and lectins complexation. Considering those previous results, we investigated the other way to make copolymer with a gradient profile and with a high hydrophobic fraction, by means of a semibatch technique

commonly used by Billon and co-workers<sup>67–70</sup> (see experiment 8 from Table 1). In this method, the S was polymerized first followed by the slow addition of the AcGalEA monomer by the mean of a pump. Figure 6 (left) showed the first-order kinetic plot of the semibatch copolymerization. For both monomers, a linear evolution with time was observed. The evolution of the molar fraction of AcGalEA in the copolymer for each sample versus the normalized chain length showed an “S-shaped” curve associated with a slight increase of the instantaneous AcGalEA molar fraction in the copolymer up to 12% (Figure 6, right).

Moreover, the evolution of number-average molar masses determined using SEC increases linearly with conversion, indicating a controlled process (Figure 7, left). The  $M_w/M_n$  of the copolymers reduces to 1.18 at 53% and 36% of conversion for respectively S and AcGalEA. SEC chromatograms showed

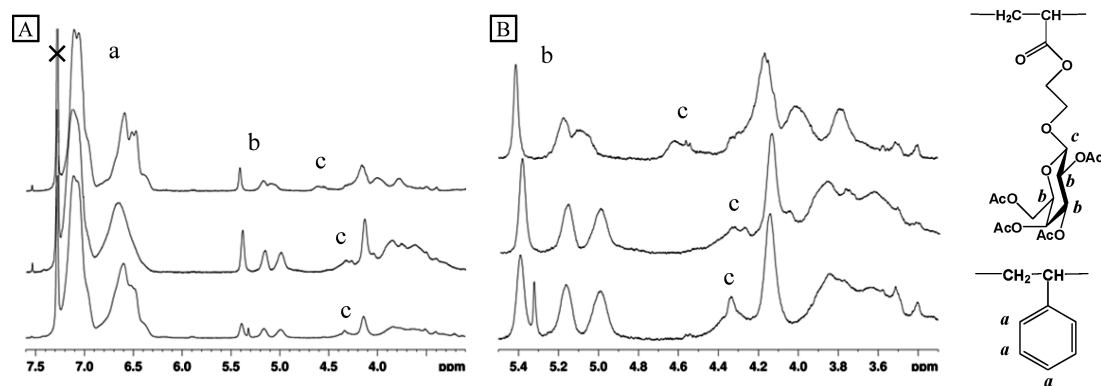


**Figure 8.**  $^1\text{H}$  NMR spectra in  $\text{CDCl}_3$  of  $\text{PACGalEA-}b\text{-PS}$  (top),  $\text{P(AcGalEA-co-S)}$  (middle), and  $\text{PS-}b\text{-P(S-grad-AcGalEA)}$  (bottom) between 3.0–7.6 ppm (A) and 3.3–5.5 ppm (B).

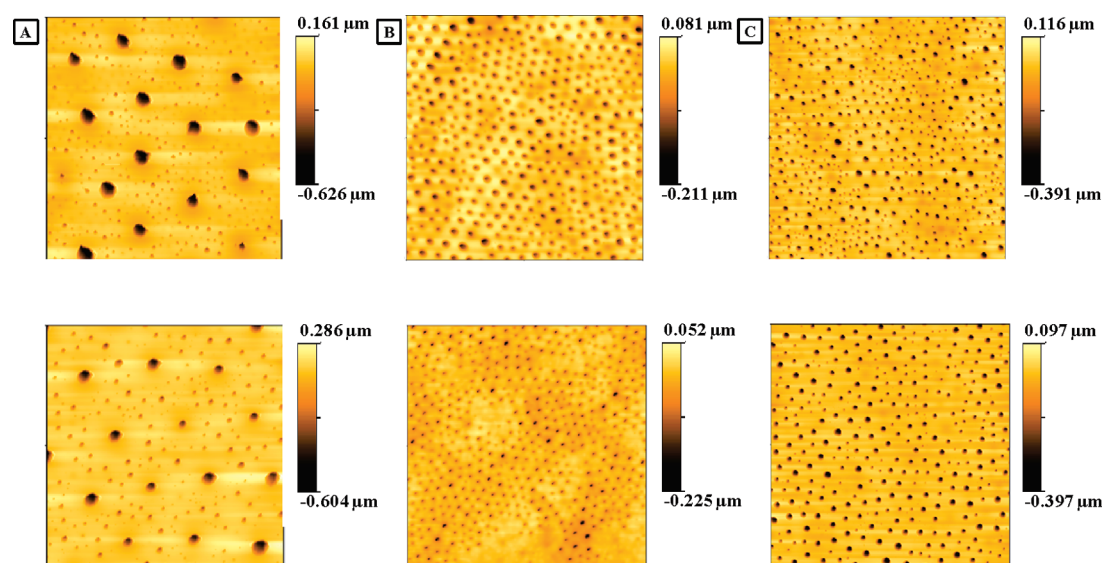


**Figure 9.** AFM topography images ( $10 \times 10 \mu\text{m}$ ) of honeycomb porous films from  $\text{PS-}b\text{-PGalEA}$ ,  $\text{PS-}b\text{-P(S-grad-GalEA)}$ , and  $\text{P(S-co-GalEA)}$  in  $\text{CS}_2$  at  $5 \text{ g L}^{-1}$  (from A to C, upper line). AFM topography images of honeycomb films obtained with mixture of  $\text{PS-}b\text{-PGalEA}$ ,  $\text{PS-}b\text{-P(S-grad-GalEA)}$ , or  $\text{P(S-co-GalEA)}$  with linear PS (1:1 w/w) (from A to C, bottom line).

closely symmetrical curves at the end of the polymerization, confirming the control of the reaction with a minimum amount of dead chains (Figure 7, right).

The influence of the synthetic methodology on macromolecular chain architecture was investigated by  $^1\text{H}$  NMR. Indeed, depending on its environment, particular effects on  $^1\text{H}$  NMR shifting for the anomeric proton of the sugar moieties were observed. Two types of signal were attributed to this anomeric proton: 4.34 and 4.31 ppm in the case of statistical and gradient profile, respectively, and a more deblinded signal at 4.62 ppm was observed in the case of block copolymer (signal *c* Figure 8A,B). The difference between the two types of signals was followed by 2D HSQC NMR experiments (see Figure SI-5 in the Supporting Information). This shift of the  $^1\text{H}$  signal for the anomeric proton was attributed to the environment of the sugar moieties. The signal at 4.62 ppm for block copolymer corresponds to  $\text{AcGalEA/AcGalEA/AcGalEA}$  triads, whereas the signal at  $\sim 4.3$  ppm for statistical and gradient copolymer corresponds to  $\text{S/AcGalEA/S}$  triads. Another consequence of the synthetic methodology on the chain architecture was observed for the  $\text{CH}$  protons from the

sugar cycle. As is shown in Figure 8A,B, the signal *b* differs from block to statistical or gradient profile. In summary, for the sugar moieties, the anomeric and  $\text{CH}$  protons from the cycle are highly sensitive to their environment. Moreover, resonances of the aromatic protons from the styrene were also affected by the environment as the profile of the spectra slightly changes for each chain architecture (Figure 8A,B).

**Deacetylation of  $\text{PS-}b\text{-PACGalEA}$ ,  $\text{P(S-co-AcGalEA)}$ , and  $\text{PS-}b\text{-P(AcGalEA-grad-S)}$  to  $\text{PS-}b\text{-PGalEA}$ ,  $\text{P(S-co-GalEA)}$ , and  $\text{PS-}b\text{-P(GalEA-grad-S)}$  Copolymers.** FT-IR and  $^1\text{H}$  NMR were employed to confirm deprotection occurred. The carbonyl band at  $1740 \text{ cm}^{-1}$  decreased sharply, and the broad hydroxyl band at  $3400 \text{ cm}^{-1}$  appeared after the deprotection (see Figure SI-6 in the Supporting Information).  $^1\text{H}$  NMR experiments of the deprotection was also confirmed by the complete disappearance of the signal from the  $\text{CH}_3$  of the protective acetyl group (at 2.10, 2.05, 1.95, and 1.6 ppm;  $4 \times \text{CH}_3$ ). Moreover, the  $\text{CH}$  signals from the sugar cycle completely disappeared, pointing out the complete deacetylation (4.98, 5.15, and 5.38 ppm) (see Figure SI-7 in the Supporting Information). Indeed, if residual

protection function were still present, the three signals should be present.

**Honeycomb Porous Films.** Syntheses of copolymers with a high hydrophobic fraction were performed in order to study their abilities to form honeycomb porous film. Atomic force microscopy (AFM) was used to observe the quality of the pores array. Images recorded in topographic mode are displayed in Figure 9. The PS-*b*-PAAcGalEA block copolymer exhibit pore sizes of 650 nm on average, with a slight irregular array. Moreover, a second porosity appears in the walls of the honeycomb film (Figure 9A, top). This second porosity was early described by Beattie et al. with PS-*b*-PAA block copolymer and was attributed to the formation of water-swollen inverse aggregates.<sup>71</sup> Wong et al. attributed this nanoporosity to the excess of water encapsulated within the pores.<sup>72</sup> Insertion of linear PS ( $M_n = 20\,000\text{ g mol}^{-1}$ ;  $M_w/M_n = 1.2$ ; 1:1 w/w) slightly enhanced the regularity of the hexagonal array, and the second porosity is still present and is perfectly distributed around the bigger pores (Figure 9A, bottom). The PS-*b*-P(S-*grad*-AcGalEA) copolymer showed a good ability to form honeycomb films as the hexagonal array formed by the pores is regular with pores ranging from 250 to 300 nm. The introduction of linear PS enables the enhancement of the regularity over a larger area (Figure 9B, top and bottom). Note that in the case of this polymer the second porosity was not present. Concerning the statistical copolymer P(S-*co*-AcGalEA), the resulting film is highly irregular with pore sizes ranging from 50 to 300 nm (Figure 9C, top). The mixture with PS poorly enhances the regularity of the array and the homogeneity of the pores diameters (Figure 9C, bottom).

## CONCLUSION

Synthesis of macromolecular chains with different architecture based on polystyrene and poly(2-(2',3',4',6'-tetra-*O*-acetyl- $\beta$ -D-galactosyloxy)ethyl acrylate) using RAFT polymerization was investigated. Moreover, the reactivity ratio of both monomers was determined using *in situ* NMR experiments. Results reveal that styrene is much more reactive than AcGalEA ( $r_S = 0.7 \pm 0.1$  and  $r_{\text{AcGalEA}} = 0.07 \pm 0.01$ ). Also, the aim of this work was to develop a new methodology for one-pot synthesis of copolymers able to create glycopolymer-based porous film. We investigated the influence of the macromolecule architecture, i.e., block, statistical, and gradient copolymers, on the honeycomb film formation by the breath figure method. Considering that a high hydrophobic fraction is required for porous film formation, the gradient profile was obtained by the mean of a pump and a semi-batch process. Nevertheless, according to the reactivity ratio, spontaneous gradient copolymer could only be obtained with a more hydrophilic character. This last gradient copolymer will be used as precursor for the formation of micelles, and these still ongoing studies will be published in a forthcoming paper.

## ASSOCIATED CONTENT

**Supporting Information.** Mass spectrometry and NMR analyses of AcGalEA monomer, plot of the AcGalEA molar fraction versus global conversion for reactivity ratio determination by the Skeist method and styrene composition profile, <sup>1</sup>H NMR and FTIR spectra for deprotection of the acetylated sugar monomer. This material is available free of charge via the Internet at <http://pubs.acs.org>.

## AUTHOR INFORMATION

### Corresponding Author

\*E-mail: laurent.billon@univ-pau.fr (L.B.); m.stenzel@unsw.edu.au (M.H.S.).

## ACKNOWLEDGMENT

Authors thank the French–Australian Science and Technology (FAST) Program FR080066 for financial support. CNRS and the French Ministry of Research are thanked for funding M. S., L.B., and L.R. Région Aquitaine is acknowledged for P.E. PhD funding. The authors also thank G. Clisson for his help on SEC analyses, H. Preud'homme for mass spectroscopy in IPREM, and I. Jacenyik and M. R. Whittaker for the management in CAMD.

## REFERENCES

- (1) Dwek, R. A. *Chem. Rev.* **1996**, *96*, 683–720.
- (2) Lis, H.; Sharon, N. *Chem. Rev.* **1998**, *98*, 637–674.
- (3) Lundquist, J. J.; Toone, E. J. *Chem. Rev.* **2002**, *102*, 555–578.
- (4) Mammen, M.; Choi, S. K.; Whitesides, G. M. *Angew. Chem., Int. Ed.* **1998**, *37*, 2755–2794.
- (5) Chen, G. J.; Tao, L.; Mantovani, G.; Geng, J.; Nystrom, D.; Haddleton, D. M. *Macromolecules* **2007**, *40*, 7513–7520.
- (6) Min, E.; Wong, K. H.; Stenzel, M. H. *Adv. Mater.* **2008**, *20*, 3550–3553.
- (7) Min, E. H.; Ting, S. R. S.; Billon, L.; Stenzel, M. H. *J. Polym. Sci., Part A: Polym. Chem.* **2010**, *48*, 3440–3455.
- (8) Ting, S. R. S.; Gregory, A. M.; Stenzel, M. H. *Biomacromolecules* **2009**, *10*, 342–352.
- (9) Ting, S. R. S.; Nguyen, T. L. U.; Stenzel, M. H. *Macromol. Biosci.* **2009**, *9*, 211–220.
- (10) Gregory, A.; Stenzel, M. H. *Expert Opin. Drug Delivery* **2011**, *8*, 237–269.
- (11) Albertin, L.; Cameron, N. R. *Macromolecules* **2007**, *40*, 6082–6093.
- (12) Albertin, L.; Kohlert, C.; Stenzel, M.; Foster, L. J. R.; Davis, T. P. *Biomacromolecules* **2004**, *5*, 255–260.
- (13) Albertin, L.; Stenzel, M.; Barner-Kowollik, C.; Foster, L. J. R.; Davis, T. P. *Macromolecules* **2004**, *37*, 7530–7537.
- (14) Albertin, L.; Stenzel, M. H.; Barner-Kowollik, C.; Davis, T. P. *Polymer* **2006**, *47*, 1011–1019.
- (15) Albertin, L.; Stenzel, M. H.; Barner-Kowollik, C.; Foster, L. J. R.; Davis, T. P. *Macromolecules* **2005**, *38*, 9075–9084.
- (16) Deng, Z. C.; Ahmed, M.; Narain, R. J. *Polym. Sci., Part A: Polym. Chem.* **2009**, *47*, 614–627.
- (17) Ladmiral, V.; Mantovani, G.; Clarkson, G. J.; Cauet, S.; Irwin, J. L.; Haddleton, D. M. *J. Am. Chem. Soc.* **2006**, *128*, 4823–4830.
- (18) Ohno, K.; Fukuda, T.; Kitano, H. *Macromol. Chem. Phys.* **1998**, *199*, 2193–2197.
- (19) Ohno, K.; Tsujii, Y.; Fukuda, T. *J. Polym. Sci., Part A: Polym. Chem.* **1998**, *36*, 2473–2481.
- (20) Ohno, K.; Tsujii, Y.; Miyamoto, T.; Fukuda, T.; Goto, M.; Kobayashi, K.; Akaike, T. *Macromolecules* **1998**, *31*, 1064–1069.
- (21) Wang, Y.; Kiick, K. L. *J. Am. Chem. Soc.* **2005**, *127*, 16392–16393.
- (22) Gordon, E. J.; Gestwicki, J. E.; Strong, L. E.; Kiessling, L. L. *Chem. Biol.* **2000**, *7*, 9–16.
- (23) Murphy, J. J.; Furusho, H.; Paton, R. M.; Nomura, K. *Chem.—Eur. J.* **2007**, *13*, 8985–8997.
- (24) Loykulnant, S.; Hirao, A. *Macromolecules* **2000**, *33*, 4757–4764.
- (25) Gotz, H.; Harth, E.; Schiller, S. M.; Frank, C. W.; Knoll, W.; Hawker, C. J. *J. Polym. Sci., Part A: Polym. Chem.* **2002**, *40*, 3379–3391.
- (26) Narumi, A.; Matsuda, T.; Kaga, H.; Satoh, T.; Kakuchi, T. *Polymer* **2002**, *43*, 4835–4840.

- (27) Narumi, A.; Satoh, T.; Kaga, H.; Kakuchi, T. *Macromolecules* **2002**, *35*, 699–705.
- (28) Ohno, K.; Izu, Y.; Yamamoto, S.; Miyamoto, T.; Fukuda, T. *Macromol. Chem. Phys.* **1999**, *200*, 1619–1625.
- (29) Ting, S. R. S.; Min, E. H.; Escale, P.; Save, M.; Billon, L.; Stenzel, M. H. *Macromolecules* **2009**, *42*, 9422–9434.
- (30) Meng, J. Q.; Du, F. S.; Liu, Y. S.; Li, Z. C. *J. Polym. Sci., Part A: Polym. Chem.* **2005**, *43*, 752–762.
- (31) Muthukrishnan, S.; Erhard, D. P.; Mori, H.; Muller, A. H. E. *Macromolecules* **2006**, *39*, 2743–2750.
- (32) Muthukrishnan, S.; Jutz, G.; Andre, X.; Mori, H.; Muller, A. H. E. *Macromolecules* **2005**, *38*, 9–18.
- (33) Muthukrishnan, S.; Mori, H.; Muller, A. H. E. *Macromolecules* **2005**, *38*, 3108–3119.
- (34) Vazquez-Dorbatt, V.; Maynard, H. D. *Biomacromolecules* **2006**, *7*, 2297–2302.
- (35) Bernard, J.; Hao, X. J.; Davis, T. P.; Barner-Kowollik, C.; Stenzel, M. H. *Biomacromolecules* **2006**, *7*, 232–238.
- (36) Lowe, A. B.; Sumerlin, B. S.; McCormick, C. L. *Polymer* **2003**, *44*, 6761–6765.
- (37) Ozyurek, Z.; Komber, H.; Gramm, S.; Schmaljohann, D.; Muller, A. H. E.; Voit, B. *Macromol. Chem. Phys.* **2007**, *208*, 1035–1049.
- (38) Pearson, S.; Allen, N.; Stenzel, M. H. *J. Polym. Sci., Part A: Polym. Chem.* **2009**, *47*, 1706–1723.
- (39) Roy, D.; Cambre, J. N.; Sumerlin, B. S. *Chem. Commun.* **2008**, *21*, 2477–2479.
- (40) Gody, G.; Boullanger, P.; Ladaviere, C.; Charreyre, M. T.; Delair, T. *Macromol. Rapid Commun.* **2008**, *29*, 511–519.
- (41) Francois, B.; Pitois, O.; Francois, J. *Adv. Mater.* **1995**, *7*, 1041–1043.
- (42) Widawski, G.; Rawiso, M.; Francois, B. *Nature* **1994**, *369*, 387–389.
- (43) Limaye, A. V.; Narhe, R. D.; Dhote, A. M.; Ogale, S. B. *Phys. Rev. Lett.* **1996**, *76*, 3762–3765.
- (44) Steyer, A.; Guenoun, P.; Beysens, D.; Knobler, C. M. *Phys. Rev. B* **1990**, *42*, 1086–1089.
- (45) Srinivasarao, M.; Collings, D.; Philips, A.; Patel, S. *Science* **2001**, *292*, 79–83.
- (46) Xu, S.; Li, M.; Mitov, Z.; Kumacheva, E. *Prog. Org. Coat.* **2003**, *48*, 227–235.
- (47) Billon, L.; Manguian, M.; Pellerin, V.; Joubert, M.; Eterradosi, O.; Garay, H. *Macromolecules* **2009**, *42*, 345–356.
- (48) Ferrari, E.; Fabbri, P.; Pilati, F. *Langmuir* **2011**, *27*, 1874–1881.
- (49) Peng, J.; Han, Y. C.; Yang, Y. M.; Li, B. Y. *Polymer* **2004**, *45*, 447–452.
- (50) Stenzel, M. H.; Barner-Kowollik, C.; Davis, T. P. *J. Polym. Sci., Part A: Polym. Chem.* **2006**, *44*, 2363–2375.
- (51) Bolognesi, A.; Botta, C.; Yunus, S. *Thin Solid Films* **2005**, *492*, 307–312.
- (52) Bunz, U. H. F. *Adv. Mater.* **2006**, *18*, 973–989.
- (53) Connal, L. A.; Franks, G. V.; Qiao, G. G. *Langmuir* **2010**, *26*, 10397–10400.
- (54) De Rosa, C.; Park, C.; Thomas, E. L.; Lotz, B. *Nature* **2000**, *405*, 433–437.
- (55) Erdogan, B.; Song, L. L.; Wilson, J. N.; Park, J. O.; Srinivasarao, M.; Bunz, U. H. F. *J. Am. Chem. Soc.* **2004**, *126*, 3678–3679.
- (56) Yunus, S.; Spano, F.; Patrinoiu, G.; Bolognesi, A.; Botta, C.; Bruhwiler, D.; Ruiz, A. Z.; Calzaferri, G. *Adv. Funct. Mater.* **2006**, *16*, 2213–2217.
- (57) Zhao, D. Y.; Feng, J. L.; Huo, Q. S.; Melosh, N.; Fredrickson, G. H.; Chmelka, B. F.; Stucky, G. D. *Science* **1998**, *279*, 548–552.
- (58) Branderhorst, H. M.; Ruijtenbeek, R.; Liskamp, R. M. J.; Pieters, R. J. *ChemBioChem* **2008**, *9*, 1836–1844.
- (59) Ting, S. R. S.; Min, E. H.; Zetterlund, P. B.; Stenzel, M. H. *Macromolecules* **2010**, *43*, 5211–5221.
- (60) Moad, G.; Rizzardo, E.; Thang, S. H. *Aust. J. Chem.* **2005**, *58*, 379–410.
- (61) Escale, P.; Save, M.; Lapp, A.; Rubatat, L.; Billon, L. *Soft Matter* **2010**, *6*, 3202–3210.
- (62) Escale, P.; Rubatat, L.; Derail, C.; Save, M.; Billon, L. *Macromol. Rapid Commun.* **2011**10.1002/marc.201100296.
- (63) Harrison, S.; Ercole, F.; Muir, B. W. *Polym. Chem.* **2010**, *1*, 326–332.
- (64) Fineman, M.; Ross, S. D. *J. Polym. Sci.* **1950**, *5*, 259–262.
- (65) Kelen, T.; Tudos, F. *J. Macromol. Sci., Chem.* **1975**, *A 9*, 1–27.
- (66) Skeist, I. *J. Am. Chem. Soc.* **1946**, *68*, 1781–1784.
- (67) Karaky, K.; Billon, L.; Pouchan, C.; Desbrieres, J. *Macromolecules* **2007**, *40*, 458–464.
- (68) Karaky, K.; Clisson, G.; Reiter, G.; Billon, L. *Macromol. Chem. Phys.* **2008**, *209*, 715–722.
- (69) Karaky, K.; Pere, E.; Pouchan, C.; Desbrieres, J.; Derail, C.; Billon, L. *Soft Matter* **2006**, *2*, 770–778.
- (70) Cherifi, N.; Issoulie, A.; Khoukh, A.; Benaboura, A.; Save, M.; Derail, C.; Billon, L. *Polym. Chem.* **2011**10.1039/C1PY00066G.
- (71) Beattie, D.; Wong, K. H.; Williams, C.; Poole-Warren, L. A.; Davis, T. P.; Barner-Kowollik, C.; Stenzel, M. H. *Biomacromolecules* **2006**, *7*, 1072–1082.
- (72) Wong, K. H.; Davis, T. P.; Barner-Kowollik, C.; Stenzel, M. H. *Polymer* **2007**, *48*, 4950–4965.